

# SCIENTIFIC REPORTS



OPEN

## Hyper-stable organo-Eu<sup>III</sup> luminophore under high temperature for photo-industrial application

Ayako Nakajima, Takayuki Nakanishi, Yuichi Kitagawa, Tomohiro Seki, Hajime Ito, Koji Fushimi & Yasuchika Hasegawa

Novel organo-Eu<sup>III</sup> luminophores, Eu(hfa)<sub>x</sub>(CPO)<sub>y</sub> and Eu(hfa)<sub>x</sub>(TCPO)<sub>y</sub> (hfa: hexafluoroacetylacetonate, CPO: 4-carboxyphenyl diphenyl phosphine oxide, TCPO: 4,4',4''-tricarboxyphenyl phosphine oxide), were synthesized by the complexation of Eu<sup>III</sup> ions with hfa moieties and CPO or TCPO ligands. The thermal and luminescent stabilities of the luminophores are extremely high. The decomposition temperature of Eu(hfa)<sub>x</sub>(CPO)<sub>y</sub> and Eu(hfa)<sub>x</sub>(TCPO)<sub>y</sub> were determined as 200 and 450 °C, respectively. The luminescence of Eu(hfa)<sub>x</sub>(TCPO)<sub>y</sub> under UV light irradiation was observed even at a high temperature, 400 °C. The luminescent properties of Eu(hfa)<sub>x</sub>(CPO)<sub>y</sub> and Eu(hfa)<sub>x</sub>(TCPO)<sub>y</sub> were estimated from emission spectra, quantum yields and lifetime measurements. The energy transfer efficiency from hfa moieties to Eu<sup>III</sup> ions in Eu(hfa)<sub>x</sub>(TCPO)<sub>y</sub> was 59%. The photosensitized luminescence of hyper-stable Eu(hfa)<sub>x</sub>(TCPO)<sub>y</sub> at 400 °C is demonstrated for future photonic applications.

There has been significant interest in the development of luminescent lanthanide materials for use in devices such as fluorescent lamps<sup>1–3</sup>, LED lights<sup>4–11</sup> and displays<sup>10–13</sup>. Recently, we have focused on organo lanthanide luminophores with strong luminescent properties for a future energy saving measures<sup>14</sup>. The organo lanthanide luminophores are attached with aromatic antenna for high photon absorption efficiency. The general organic luminophores are decomposed under 200 °C unfortunately. In the case of industrial applications of organic devices using luminescent lanthanide materials, thermostability is required for effective material production process and long term durability. This manuscript describes new organo lanthanide luminophores with thermostability and strong luminescent properties using a photosensitized effect. The organo lanthanide luminophore at 400 °C is inconceivable material, which is put on a characteristics of solid ceramics and smart molecules.

There are currently various types of organo lanthanide luminophores based on characteristic ligand design that have been developed as strongly luminescent materials<sup>14–35</sup>. A three-dimensional networks composed of organo lanthanide luminophores, which prevent stretching vibration and rotations of organic ligands, leads to a thermostable structure. Du and coworkers have synthesized a three-dimensional lanthanide compound with 1,3-benzenedicarboxylic acid for the construction of a thermostable structure<sup>36</sup>. Hong and coworkers have demonstrated that a three-dimensional lanthanide metal-organic framework (MOF) composed of lanthanide ions (Ln<sup>III</sup> = Nd, Sm, Eu, Gd) and tris-(4-carboxylphenyl)phosphine oxide has a high decomposition temperature (500 °C)<sup>37</sup>. However, the benzene-typed joint ligands do not promote effective photosensitization in organo-Eu<sup>III</sup> luminophores ( $\eta < 1\%$ ). Thermostable lanthanide luminophores with effective photosensitization are expected to open up a new field of luminescent material science. We have attempted to prepare an organo lanthanide material with high thermostability and effective photosensitized luminescence. In this study, novel organo-Eu<sup>III</sup> luminophores with hfa moieties (hfa: hexafluoroacetylacetonato) and carboxy phosphine oxide (CPO: 4-carboxyphenyl diphenyl phosphine oxide/TCPO: 4,4',4''-tricarboxyphenyl phosphine oxide) are reported, the structures of which are shown in Fig. 1. The hfa moieties act as photosensitization ligands in organo-Eu<sup>III</sup> luminophores and play an important role in the suppression of non-radiative transition via vibrational relaxation due to their lower vibrational frequencies<sup>38</sup>. Coordination of the phosphine oxide parts in CPO and TCPO as three-dimensional joint ligands provides a low-vibrational frequency for strong luminescence. The CPO and TCPO ligands are also

Faculty of Engineering, Hokkaido University, N13 W8, Kita-ku, Sapporo, Hokkaido 060-8626, Japan. Correspondence and requests for materials should be addressed to Y.H. (email: hasegaway@eng.hokudai.ac.jp)

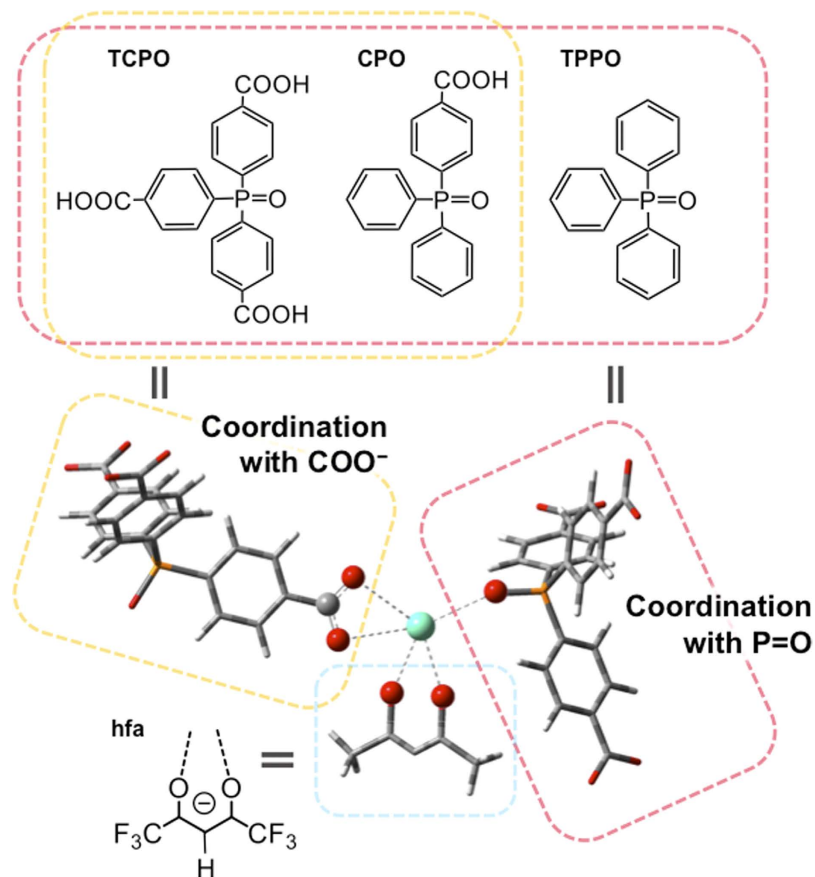


**Figure 1.** Structural images of  $\text{Eu}^{\text{III}}$  luminophore,  $\text{Eu}(\text{hfa})_x(\text{TCPO})_y$ ,  $\text{Eu}(\text{hfa})_x(\text{CPO})_y$  and  $\text{Eu}(\text{hfa})_3(\text{TPPO})_2$  described using GaussView 5.0.

designed to include carboxy groups for construction of the thermostable Ln-MOF structure reported by Hong and coworkers<sup>37</sup>. A mononuclear  $\text{Eu}^{\text{III}}$  complex,  $\text{Eu}(\text{hfa})_3(\text{TPPO})_2$  (TPPO: triphenylphosphine oxide) was prepared as a standard reference. The thermostability of the organo- $\text{Eu}^{\text{III}}$  luminophores was evaluated using thermogravimetric analysis (TGA). The luminescent properties were estimated from emission spectra, quantum yields and lifetime measurements. The bright luminescence of  $\text{Eu}(\text{hfa})_x(\text{TCPO})_y$  at 400 °C was successfully observed and the energy transfer efficiency of  $\text{Eu}(\text{hfa})_x(\text{TCPO})_y$  was calculated to be 47%. Thus, thermostable and effective photosensitized organo- $\text{Eu}^{\text{III}}$  luminophores were demonstrated for the first time.

## Results and Discussion

**Thermostable Properties.** In previous work,  $\text{Eu}^{\text{III}}$  luminophore with carboxy phosphine oxide have been reported<sup>37</sup>. The material has no photosensitized hfa moiety.  $\text{Eu}(\text{hfa})_x(\text{TCPO})_y$  and  $\text{Eu}(\text{hfa})_x(\text{CPO})_y$  were synthesized by the complexation of the carboxy phosphine oxide (CPO or TCPO) with  $\text{Eu}(\text{hfa})_3(\text{H}_2\text{O})_2$  in methanol under reflux. The phosphine oxide parts ( $\text{P}=\text{O}$ ) and the carboxy groups ( $\text{COO}^-$ ) in CPO and TCPO ligands effectively promote the formation of polymeric structures. The significant vibrational bands at  $\text{C}=\text{O}$  and  $\text{P}=\text{O}$  groups of  $\text{Eu}(\text{hfa})_x(\text{CPO})_y$  were shifted to shorten wavenumbers ( $1658$  and  $1143\text{ cm}^{-1}$ ) (CPO ligand:  $1702$  and  $1151\text{ cm}^{-1}$ ). The IR bands of  $\text{Eu}(\text{hfa})_x(\text{TCPO})_y$  were also observed at  $1622$  and  $1102\text{ cm}^{-1}$ , which are shorter than those of the ligand (TCPO ligand:  $1692$  and  $1115\text{ cm}^{-1}$ ) (see Supplementary Information, Fig. S1). We successfully synthesized  $\text{Eu}(\text{hfa})_x(\text{TCPO})_y$  without base condition. This chelate reaction is a new method for preparation of  $\text{Eu}(\text{hfa})_x(\text{TCPO})_y$ . On the other hand,  $\text{Eu}(\text{hfa})_x(\text{CPO})_y$  is prepared under base-condition (addition of triethyl amine). The reaction difference is might be due to moiety of the joint ligands, CPO and TCPO. The  $x$  and  $y$  in formulas in  $\text{Eu}(\text{hfa})_x(\text{CPO})_y$  and  $\text{Eu}(\text{hfa})_x(\text{TCPO})_y$  are defined  $0 < x < 1$  and  $0 < y < 3$ . We estimated  $x = 0.38$ ,  $y = 2.12$  in  $\text{Eu}(\text{hfa})_x(\text{CPO})_y$  and  $x = 0.03$ ,  $y = 1.92$  in  $\text{Eu}(\text{hfa})_x(\text{TCPO})_y$  using EDX data (see Supplementary Information, Fig. S2). In order to identify the structure of  $\text{Eu}(\text{hfa})_x(\text{TCPO})_y$ , we tried to measure by single-crystal X-ray structure analysis. The structure was determined to be eight-coordinated structure with two water molecules and five TCPO ligands. The two TCPO ligands show bidentate bridged connection between two  $\text{Eu}^{\text{III}}$  ions (TCPO A in Fig. 2). We also found that two TCPO ligands show bidentate (TCPO B) and monodentate (TCPO C) connection in one  $\text{Eu}^{\text{III}}$  ion. Final TCPO ligand is attached to one  $\text{Eu}^{\text{III}}$  ion by  $\text{P}=\text{O}$  group (TCPO D). The  $\text{Eu}(\text{hfa})_x(\text{TCPO})_y$  crystal provides three dimensional network structure. This single crystal is including four methanol molecules in one unit (Fig. 2 and Table 1). These structures of the polymeric compounds were analyzed using X-ray diffraction (XRD) measurements. Figure 3 shows XRD patterns for both luminophores. Broad peaks were observed for  $\text{Eu}(\text{hfa})_x(\text{CPO})_y$  at around  $20^\circ$  and  $28^\circ$  (Fig. 3a). The  $\text{Eu}(\text{hfa})_x(\text{CPO})_y$  has

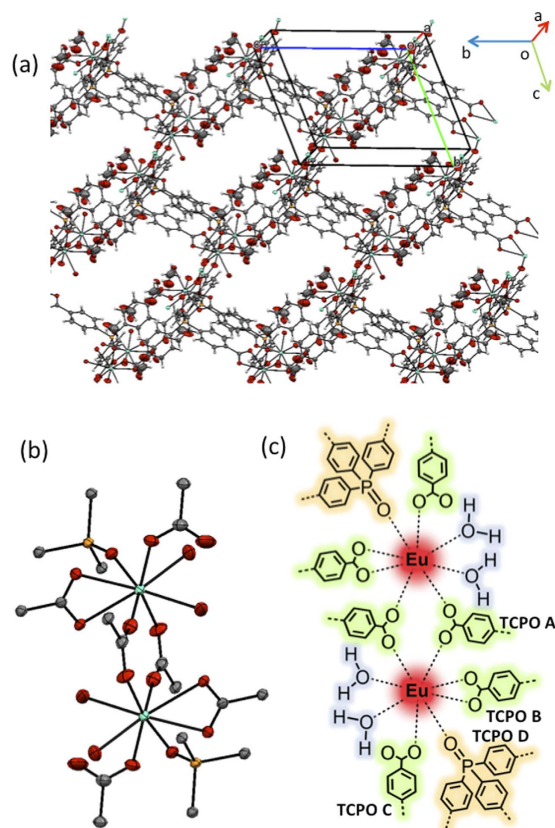


**Figure 2.** (a,b) ORTEP views of  $\text{Eu}(\text{hfa})_x(\text{TCPO})_y$  consisted of  $\text{Eu}^{\text{III}}$  ions and TCPO ligands, (c) chemical structure of  $\text{Eu}^{\text{III}}$  coordination sites.

Chemical formula	$\text{C}_{22.32}\text{H}_{17.28}\text{EuO}_{10.6}\text{P}$
Formula weight	638.03
Crystal system	Triclinic
Space group	$P-1(\#2)$
$a/\text{\AA}$	10.7020(3)
$b/\text{\AA}$	12.0041(3)
$c/\text{\AA}$	14.5272(4)
$\alpha/\text{deg}$	112.456(2)
$\beta/\text{deg}$	94.940(2)
$\gamma/\text{deg}$	101.867(2)
Volume/ $\text{\AA}^3$	1659.69(8)
Z	2
$d_{\text{calc}}/\text{g cm}^{-3}$	1.277
Temperature/ $^{\circ}\text{C}$	-180
$\mu$ (Mo $\text{K}\alpha$ )/ $\text{cm}^{-1}$	19.747
max $2\theta/\text{deg}$	55.0
Reflections collected	30169
Independent reflections	7550
$R_1$	0.0325
$wR_2$	0.0847

**Table 1.** Crystallographic data for  $\text{Eu}(\text{hfa})_x(\text{TCPO})_y$ . [a]  $R_1 = \sum ||F_o| - |F_c|| / \sum |F_o|$ . [b]  $wR_2 = [\sum w (F_o^2 - F_c^2)^2 / \sum w (F_o^2)^2]$ .

an amorphous structure at room temperature. In contrast, the as-prepared white powder of  $\text{Eu}(\text{hfa})_x(\text{TCPO})_y$  has noticeable peaks at  $11.29^\circ$ ,  $12.41^\circ$ ,  $13.45^\circ$ ,  $14.76^\circ$ ,  $18.88^\circ$ ,  $19.47^\circ$ ,  $22.62^\circ$ ,  $23.44^\circ$ ,  $24.23^\circ$ ,  $25.41^\circ$ ,  $28.48^\circ$ , and  $30.11^\circ$  (Fig. 3b), and  $\text{Eu}(\text{hfa})_x(\text{TCPO})_y$  after heat treatment ( $90^\circ\text{C}$ , 2 h, under reduced pressure) also has

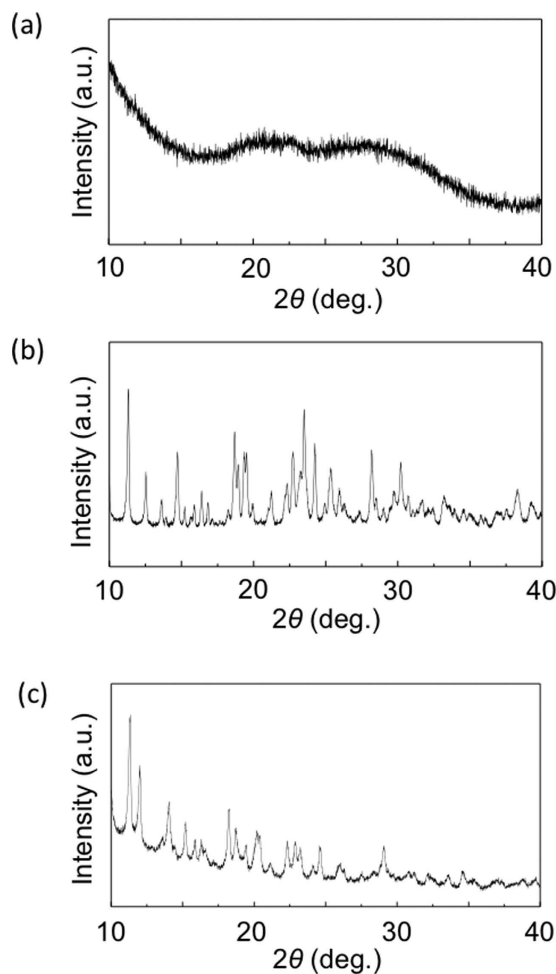


**Figure 3.** XRD patterns of (a)  $\text{Eu}(\text{hfa})_x(\text{CPO})_y$ , (b) as-prepared  $\text{Eu}(\text{hfa})_x(\text{TCPO})_y$  and (c)  $\text{Eu}(\text{hfa})_x(\text{TCPO})_y$  under heat treatment at  $90^\circ\text{C}$ .

noticeable peak at  $11.32^\circ$ ,  $11.99^\circ$ ,  $14.05^\circ$ ,  $15.21^\circ$ ,  $18.22^\circ$ ,  $18.73^\circ$ ,  $20.21^\circ$ ,  $20.37^\circ$ ,  $22.29^\circ$ ,  $22.88^\circ$ ,  $23.23^\circ$ , and  $29.07^\circ$  (Fig. 3c). Thus, it is considered that the triphenylphosphine oxide with three carboxy groups, the TCPO joint ligand, leads to the formation of a crystalline structure, and the structure change by heat treatment. We have checked the XRD of  $\text{Eu}(\text{hfa})_x(\text{TCPO})_y$  compared with that of  $\text{Eu}((\text{CH}_3)_2\text{NCHO})_x(\text{TCPO})_y$  in previous work<sup>37</sup> (see Supplementary Information, Fig. S3). The XRD patterns of  $\text{Eu}(\text{hfa})_x(\text{TCPO})_y$  is much different from that of  $\text{Eu}((\text{CH}_3)_2\text{NCHO})_x(\text{TCPO})_y$ . Identification of the polymeric structure was performed using fast atom bombardment-mass spectrometry (FAB-MS) and energy dispersive X-ray spectroscopy (EDX) measurements. The fragment peaks of  $\text{Eu}(\text{hfa})_x(\text{CPO})_y$  and  $\text{Eu}(\text{hfa})_x(\text{TCPO})_y$  in the FAB-MS spectra agree with those calculated for  $[\text{Eu}_2(\text{hfa})_3(\text{CPO})_2]^+$  and  $[\text{Eu}(\text{hfa})_2(\text{TCPO})\cdot 5\text{H}_2\text{O}]^+$  fragments, respectively (see Supplementary Information Fig. S4). According to the determination of element ratio, we estimated the  $\text{Eu}(\text{M}\alpha)$ ,  $\text{P}(\text{K}\alpha)$  and  $\text{F}(\text{K}\alpha)$  of  $\text{Eu}(\text{hfa})_x(\text{CPO})_y$  and  $\text{Eu}(\text{hfa})_x(\text{TCPO})_y$  for EDX measurements calibrated with  $\text{Eu}(\text{hfa})_3(\text{TPPO})_2$  as a standard. The EDX measurements indicated the percentage of hfa moieties in  $\text{Eu}(\text{hfa})_x(\text{CPO})_y$  and  $\text{Eu}(\text{hfa})_x(\text{TCPO})_y$  were 10.8% and 0.89%, respectively. We propose that the small amount of hfa molecules attached on the crystal surface. The hfa molecules on the surface were successfully detected by ionized-fragment information using FAB-MS spectrum (Fig. S4b  $\text{Eu}(\text{hfa})_2\text{TCPO}\cdot 5\text{H}_2\text{O}$ ). In contrast, the EDX signals of the XRF measurement gave the average information about total element ratio of  $\text{Eu}(\text{hfa})_x(\text{TCPO})_y$ .

The thermo-stabilities of the  $\text{Eu}(\text{hfa})_x(\text{CPO})_y$  and  $\text{Eu}(\text{hfa})_x(\text{TCPO})_y$  polymeric structures were evaluated using TGA and the results are shown in Fig. 4. The TGA profile for the luminescent mononuclear  $\text{Eu}^{\text{III}}$  complex,  $\text{Eu}(\text{hfa})_3(\text{TPPO})_2$ , was also measured as a standard reference. The decomposition temperature of  $\text{Eu}(\text{hfa})_3(\text{TPPO})_2$  was  $200^\circ\text{C}$ . The weight of  $\text{Eu}(\text{hfa})_x(\text{CPO})_y$  gradually decreases from  $200^\circ\text{C}$ , which may be due to the loose packing structure in amorphous  $\text{Eu}(\text{hfa})_x(\text{CPO})_y$  to promote partial elimination of the hfa moieties. The decomposition temperature of  $\text{Eu}(\text{hfa})_x(\text{TCPO})_y$  was  $450^\circ\text{C}$ . We cannot observed the elimination of solvent from the material. This result indicates that  $\text{Eu}(\text{hfa})_x(\text{TCPO})_y$  have no solvent in the structure after heat treatment. Therefore, XRD measurements of  $\text{Eu}(\text{hfa})_x(\text{TCPO})_y$  were kept under  $450^\circ\text{C}$  (see Supplementary Information, Fig. S5). The decomposition temperature of  $\text{Eu}(\text{hfa})_x(\text{TCPO})_y$  is the highest among the organo- $\text{Eu}^{\text{III}}$  luminophores with photosensitized hfa moieties. Thus, a luminescent organo- $\text{Eu}^{\text{III}}$  luminophore with extra-high thermostability was successfully synthesized.

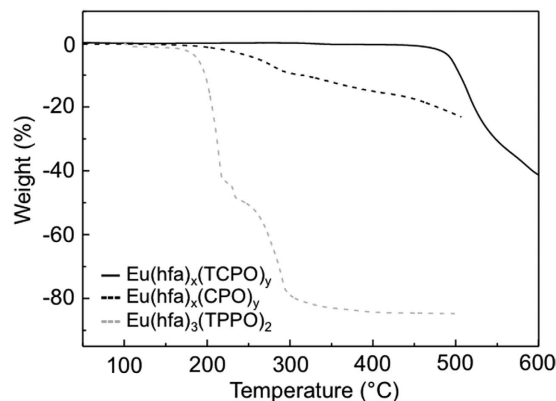


**Figure 4.** TGA profiles of  $\text{Eu}(\text{hfa})_x(\text{TCPO})_y$  (black line),  $\text{Eu}(\text{hfa})_x(\text{CPO})_y$  (black dot line), and  $\text{Eu}(\text{hfa})_3(\text{TPPO})_2$  (gray dot line) under an argon atmosphere.

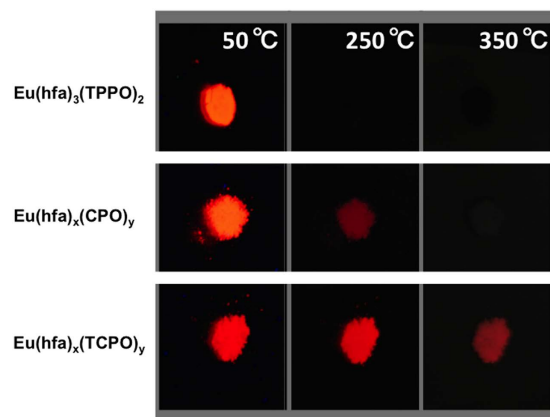


**Figure 5.** Photographs of  $\text{Eu}(\text{hfa})_3(\text{TPPO})_2$ ,  $\text{Eu}(\text{hfa})_x(\text{CPO})_y$  and  $\text{Eu}(\text{hfa})_x(\text{TCPO})_y$  at 50 °C, 250 °C, and 350 °C heating on the hot plate under UV light irradiation ( $\lambda = 365 \text{ nm}$ ).

The luminescence images for  $\text{Eu}(\text{hfa})_3(\text{TPPO})_2$ ,  $\text{Eu}(\text{hfa})_x(\text{CPO})_y$  and  $\text{Eu}(\text{hfa})_x(\text{TCPO})_y$  heated on a hot plate under UV light irradiation ( $\lambda = 365 \text{ nm}$ ) are shown in Fig. 5.  $\text{Eu}(\text{hfa})_3(\text{TPPO})_2$  exhibits red luminescence at 50 °C but does not emit photons at 250 °C due to their thermal decomposition. The red luminescence of  $\text{Eu}(\text{hfa})_x(\text{CPO})_y$  faded out at around 250 °C. In contrast, bright red luminescence was successfully observed from  $\text{Eu}(\text{hfa})_x(\text{TCPO})_y$  under 400 °C. (See emission spectra under control of temperature in Supplementary Information, Fig. S6a). Thus,  $\text{Eu}(\text{hfa})_x(\text{TCPO})_y$  exhibits both effective photosensitized luminescence and thermostability.

**Luminescent Properties.** Excitation and emission spectra for  $\text{Eu}(\text{hfa})_3(\text{TPPO})_2$ ,  $\text{Eu}(\text{hfa})_x(\text{CPO})_y$  and  $\text{Eu}(\text{hfa})_x(\text{TCPO})_y$  in the solid state detected at 613.5 nm and excited at 365 nm are shown in Fig. 6. The excitation bands of  $\text{Eu}(\text{hfa})_x(\text{CPO})_y$  at around 300 nm is assigned to  $\pi-\pi^*$  transition of hfa moieties<sup>39</sup>. We also found characteristic excitation band at around 400 nm in  $\text{Eu}(\text{hfa})_x(\text{TCPO})_y$  crystals. The emission bands were observed at around 578, 591, 613, 651, and 699 nm, which are attributed to the  $4f-4f$  transitions of  $\text{Eu}^{\text{III}}$  ( $^5\text{D}_0-^7\text{F}_j$ ;  $J = 0, 1, 2, 3, \text{ and } 4$ , respectively). The spectra were normalized with respect to the magnetic dipole transition intensities at 591 nm ( $\text{Eu}^{\text{III}}$ ;  $^5\text{D}_0-^7\text{F}_1$ ), which is known to be insensitive to the surrounding environment of the lanthanide ions. The normalized emission intensity of  $\text{Eu}(\text{hfa})_x(\text{TCPO})_y$  at 613 nm is larger than that of  $\text{Eu}(\text{hfa})_x(\text{CPO})_y$ . These spectral shapes of  $\text{Eu}(\text{hfa})_x(\text{TCPO})_y$  and  $\text{Eu}(\text{hfa})_x(\text{CPO})_y$  are different from that of crystalline  $\text{Eu}(\text{hfa})_3(\text{TPPO})_2$ .

Time-resolved emission profiles of  $\text{Eu}(\text{hfa})_x(\text{CPO})_y$  and  $\text{Eu}(\text{hfa})_x(\text{TCPO})_y$  are shown in Fig. 6b,c, respectively. The emissions from  $\text{Eu}(\text{hfa})_x(\text{CPO})_y$  indicates single-exponential decays of millisecond scale. We estimated the emission lifetime of  $\text{Eu}(\text{hfa})_x(\text{TCPO})_y$  using single-exponential decay. The lifetime and  $R^2$  under single-exponential analysis were found to be 0.61 ms and 0.996, respectively. The lifetime is similar to that of  $\text{Eu}(\text{hfa})_x(\text{CPO})_y$ . In this paper, we used the single-exponential analysis for estimation of lifetime of  $\text{Eu}(\text{hfa})_x(\text{TCPO})_y$ . We consider that the luminescence of  $\text{Eu}(\text{hfa})_x(\text{TCPO})_y$  comes from one-dominant  $\text{Eu}^{\text{III}}$  species with hfa moieties on the crystal surface. The emission lifetimes of  $\text{Eu}(\text{hfa})_3(\text{TPPO})_2$ ,  $\text{Eu}(\text{hfa})_x(\text{CPO})_y$  and  $\text{Eu}(\text{hfa})_x(\text{TCPO})_y$  were determined to be 0.80, 0.60 and 0.61 ms, respectively.

The  $4f-4f$  emission quantum yields ( $\Phi_{4f-4f}$ ) and the radiative ( $k_r$ ) and non-radiative ( $k_{nr}$ ) rate constants of these  $\text{Eu}^{\text{III}}$  compounds were calculated using the following equations.

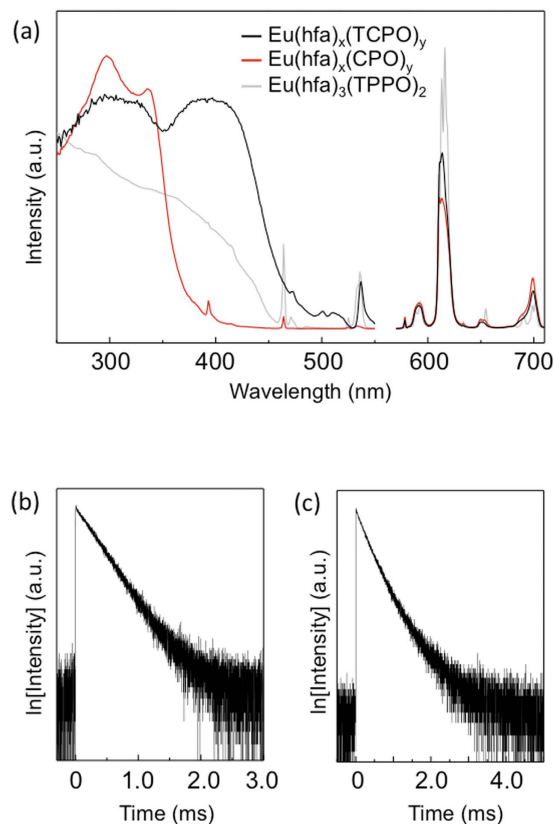


**Figure 6.** (a) Excitation and Emission spectra of  $\text{Eu}(\text{hfa})_x(\text{TCPO})_y$  (black line),  $\text{Eu}(\text{hfa})_x(\text{CPO})_y$  (red line) and  $\text{Eu}(\text{hfa})_3(\text{TPPO})_2$  (gray line) excited at 365 nm in the solid state, Decay profile of (b)  $\text{Eu}(\text{hfa})_x(\text{CPO})_y$  and (c)  $\text{Eu}(\text{hfa})_x(\text{TCPO})_y$  in the solid state.

$$\frac{1}{\tau_{\text{rad}}} = A_{\text{MD},0} n^3 \left( \frac{I_{\text{tot}}}{I_{\text{MD}}} \right) \quad (1)$$

$$\Phi_{4f-4f} = \frac{k_r}{k_r + k_{\text{nr}}} = \frac{\tau_{\text{obs}}}{\tau_{\text{rad}}} \quad (2)$$

$$k_r = \frac{1}{\tau_{\text{rad}}} \quad (3)$$

$$k_{\text{nr}} = \frac{1}{\tau_{\text{obs}}} - \frac{1}{\tau_{\text{rad}}} \quad (4)$$

The radiative lifetime ( $\tau_{\text{rad}}$ ) is defined as an ideal emission lifetime without non-radiative processes. The radiative lifetime is expressed by equation 1, where  $A_{\text{MD},0}$  is the spontaneous emission probability for the  $^5\text{D}_0-^7\text{F}_1$  transition *in vacuo* ( $14.65 \text{ s}^{-1}$ ),  $n$  is the refractive index of the medium (an average index of refraction equal to 1.5 was employed), and  $(I_{\text{tot}}/I_{\text{MD}})$  is the ratio of the total area of the corrected  $\text{Eu}^{\text{III}}$  emission spectrum to the area of the  $^5\text{D}_0-^7\text{F}_1$  band. The emission quantum yields, and the radiative and non-radiative rate constants are summarized in Table 2.

The emission quantum yield of  $\text{Eu}(\text{hfa})_x(\text{TCPO})_y$  excited at 355 nm ( $\Phi_{\pi-\pi^*}: \pi-\pi^*$  transition band of hfa moieties) was also measured to calculate the energy transfer efficiency ( $\eta$ ), which was determined as 34%. The energy transfer efficiency of  $\text{Eu}(\text{hfa})_x(\text{TCPO})_y$  (decomposition temperature = 450 °C,  $\eta = 59\%$ ) is larger than that of the previously reported thermostable organo- $\text{Eu}^{\text{III}}$  luminophore,  $[\text{Eu}(\text{hfa})_3(\text{dppb})]_n$  (dppb: 4,4'-bis(diphenyl phosphonyl)biphenyl, decomposition temperature = 308 °C,  $\eta = 40\%$ )<sup>40</sup>.

## Summary and Conclusions

A organo- $\text{Eu}^{\text{III}}$  luminophore,  $\text{Eu}(\text{hfa})_x(\text{TCPO})_y$ , with effective thermostability and photosensitized luminescent property was successfully synthesized. Thermostable  $\text{Eu}(\text{hfa})_x(\text{TCPO})_y$  exhibits bright red luminescence at 400 °C under UV light irradiation. The luminescence of  $\text{Eu}(\text{hfa})_x(\text{TCPO})_y$  is due to photosensitized energy transfer from

	Td (°C)	$\tau_{\text{obs}}$ (ms)	$\tau_{\text{rad}}$ (ms)	$\tau_{\text{diff}}$ (%)	$k_r$ (s <sup>-1</sup> )	$k_{nr}$ (s <sup>-1</sup> )	$\Phi_{\pi-\pi^*}$ (%)	$\eta$ (%)
Eu(hfa) <sub>3</sub> (TPPO) <sub>2</sub>	200	0.80	1.23	65	$8.1 \times 10^2$	$4.4 \times 10^2$	51	78
Eu(hfa) <sub>3</sub> (dpbp)	308	0.85	1.20	72	$8.5 \times 10^2$	$3.2 \times 10^2$	29	40
Eu(hfa) <sub>x</sub> (CPO) <sub>y</sub>	200	0.60	2.13	28	$4.7 \times 10^2$	$1.2 \times 10^3$	15	54
Eu(hfa) <sub>x</sub> (TCPO) <sub>y</sub>	450	0.61	1.77	34	$5.7 \times 10^2$	$1.1 \times 10^3$	20	59

**Table 2. Photophysical properties of each complexes in the solid state.** Td is decomposition temperature.  $\Phi_{\pi-\pi^*}$  is emission quantum yield excited at 355 nm.  $\eta$  is energy transfer efficiency from hfa moieties to Eu<sup>III</sup> ions. Eu(hfa)<sub>3</sub>(TPPO)<sub>2</sub>; see ref. 39. Eu(hfa)<sub>3</sub>(dpbp); see ref. 40.

hfa moieties to Eu<sup>III</sup> ions. Thermostable organo-lanthanide luminophores are expected to open up the frontier fields of photophysical science, material chemistry and industrial applications.

## Experimental Section

**Materials.** Europium acetate *n*-hydrate (99.9%), diphenyl(*p*-tolyl)phosphine and tri-*p*-tolylphosphine were purchased from Wako Pure Chemical Industries Ltd. Hexafluoroacetylacetone and triphenylphosphine oxide (TPPO) were obtained from Tokyo Kasei Organic Chemicals Co., Inc. Dimethyl sulfoxide-*d*<sub>6</sub> (D, 99.9%) was obtained from Kanto Chemical Co., Inc. All other chemicals and solvents were reagent grade and were used without further purification.

**Apparatus.** <sup>1</sup>H NMR (400 MHz) spectra were recorded on a JEOL ECS400. Chemical shifts were reported in  $\delta$  ppm, referenced to an internal tetramethylsilane standard for <sup>1</sup>H NMR spectroscopy. Infrared spectra were measured using a Thermo Nicolet AVATAR 320 FT-IR spectrometer. FAB-MS spectra were recorded on a JEOL JMS-700TZ. Elemental analyses were performed on a J-Science Lab Micro Corder JM 10 and an Exeter Analytical CE440. In addition, the ratio of F to Eu was measured using Energy Dispersive X-ray Fluorescence Spectrometer EDX-8000 with (reference material: Eu(hfa)<sub>3</sub>(TPPO)<sub>2</sub>). XRD patterns were characterized by a RIGAKU SmartLab X-ray diffractometer with Cu K $\alpha$  radiation, a D/teX Ultra detector, and a temperature control unit (Anton Paar, TCU-110). Thermogravimetric Analysis was performed on a Seiko Instruments Inc. EXSTAR 6000 (TG-DTA 6300) at first heating rate of 10 °C min<sup>-1</sup> up to 100 °C, cooling rate of 10 °C min<sup>-1</sup> up to 40 °C, and second heating rate of 1 °C min<sup>-1</sup> up to 500 °C.

**Preparation of 4-carboxyphenyl diphenyl phosphine oxide (CPO).** CPO was synthesized by the oxidation of diphenyl(*p*-tolyl)phosphine with potassium permanganate, according to the procedure described in the literature<sup>41</sup>. Yield: 54%; <sup>1</sup>H NMR (400 MHz, DMSO-*d*<sub>6</sub>, 298K):  $\delta$  8.10–8.06 (*dd*, 2H), 7.78–7.72 (*dd*, 2H), 7.67–7.61 (*m*, 6H), 7.60–7.54 (*td*, 4H) ppm; IR (ATR): 1658, 1592, 1540, 1498, 1411, 1254, 1144, 1118 cm<sup>-1</sup>; Elemental analysis calcd (%) for C<sub>19</sub>H<sub>15</sub>O<sub>3</sub>P: C 70.81, H 4.69; found: C 70.15, H 4.49.

**Preparation of 4,4',4''-tricarboxyphenyl phosphine oxide (TCPO).** TCPO was synthesized by the oxidation of tri-*p*-tolylphosphine with potassium permanganate, according to the procedure described in the literature<sup>42</sup>. Yield: 34%; <sup>1</sup>H NMR (400 MHz, DMSO-*d*<sub>6</sub>, 298K):  $\delta$  8.12–8.08 (*dd*, 6H), 7.88–7.75 (*dd*, 6H) ppm; IR (ATR): 1692, 1395, 1246, 1162, 1102, 1016 cm<sup>-1</sup>; Elemental analysis calcd (%) for [C<sub>21</sub>H<sub>15</sub>O<sub>7</sub>P + H<sub>2</sub>O]: C 58.89, H 4.00; found: C 58.67, H 4.08.

**Preparation of [Eu(hfa)<sub>3</sub>(H<sub>2</sub>O)<sub>2</sub>].** Europium acetate *n*-hydrate (5.0 g, 12 mmol) was dissolved in distilled water (20 mL). A solution of hexafluoroacetylacetone was added dropwise to the solution. The reaction mixture produced a precipitation of white yellow powder after stirring for 3 h at room temperature. The reaction mixture was filtered, and the resulting powder was used without further purification for next step. Yield: 95%; IR (KBr): 1650, 1258–1145 cm<sup>-1</sup>; Elemental analysis calcd (%) for C<sub>15</sub>H<sub>7</sub>EuF<sub>18</sub>O<sub>8</sub>: C 22.27, H 0.87; found: C 22.12, H 1.01<sup>42,43</sup>.

**Preparation of Eu(hfa)<sub>3</sub>(TPPO)<sub>2</sub>.** Methanol (100 mL) containing Eu(hfa)<sub>3</sub>(H<sub>2</sub>O)<sub>2</sub> (4.28 g, 6 mmol) and TPPO (2.78 g, 10 mmol) was refluxed under stirring for 12 h. The reaction mixture was concentrated using a rotary evaporator. Recrystallization by addition of excess hexane solution produced crude crystal, which were washed in toluene several times. Recrystallization from hot toluene/cyclohexane gave white needle crystals. Yield: 74%; <sup>1</sup>H-NMR (400 MHz, CD<sub>3</sub>-COCD<sub>3</sub>, TMS):  $\delta$  = 5.42 (*s*, 3H), 7.58–7.71 (*m*, 12H), 7.76–7.86 (*m*, 6H), 8.67 (*br*, 12H) ppm; IR (KBr): 1650, 1250–1150, 1125 cm<sup>-1</sup>; Elemental analysis calcd (%) for C<sub>51</sub>H<sub>33</sub>EuF<sub>18</sub>O<sub>8</sub>P<sub>2</sub>: C 46.07, H 2.50; found: C 45.94, H 2.57<sup>38</sup>.

**Preparation of Eu(hfa)<sub>x</sub>(CPO)<sub>y</sub>.** CPO (207 mg, 0.64 mmol) and Eu(hfa)<sub>3</sub>(H<sub>2</sub>O)<sub>2</sub> (720 mg, 0.89 mmol) were dispersed in methanol (30 mL), and triethylamine was added to neutralize. The dispersion was stirred for 5 h at 60 °C. The precipitate was washed with methanol several times, and dried *in vacuo*. Yield: 45.3 mg; IR (ATR) 1658, 1592, 1540, 1498, 1411, 1254, 1144, 1118 cm<sup>-1</sup>; FAB-MS (*m/z*): [Eu<sub>2</sub>(hfa)<sub>3</sub>(CPO)<sub>2</sub>]<sup>+</sup> calcd for C<sub>53</sub>H<sub>31</sub>Eu<sub>2</sub>F<sub>18</sub>O<sub>12</sub>P<sub>2</sub>, 1566.9; found 1566.7; EDX found (%): CPO, 60.0; Eu, 28.3; hfa, 10.7.

**Preparation of Eu(hfa)<sub>x</sub>(TCPO)<sub>y</sub>.** TCPO (260 mg, 0.63 mmol) and Eu(hfa)<sub>3</sub>(H<sub>2</sub>O)<sub>2</sub> (720 mg, 0.89 mmol) were dispersed in methanol (30 mL). The dispersion was stirred for 9 h at 60 °C. The white precipitate was washed with methanol several times, and dried *in vacuo* oven at 90 °C (see Supplementary Information, Fig. S8).

Yield: 294.7 mg; IR (ATR) 1624, 1548, 1398, 1382, 1185, 1145, 1116, 1050, 1018  $\text{cm}^{-1}$ ; FAB-Mass (m/z):  $[\text{Eu}(\text{hfa})_2(\text{TCPO})\cdot 5\text{H}_2\text{O}]^+$  calcd for  $\text{C}_{31}\text{H}_{27}\text{EuF}_{12}\text{O}_{16}\text{P}$ , 1067.01; found 1067.3; EDX found (%): TCPO, 64.9; Eu, 33.8; hfa, 0.9.

**Optical measurements.** Emission spectra were recorded on a HORIBA Fluorolog-3 spectrofluorometer and corrected for the response of the detector system. Emission lifetimes ( $\tau_{\text{obs}}$ ) were measured using the third harmonics (355 nm) of a Q-switched Nd:YAG laser (Spectra Physics, INDI-50,  $\text{fwhm} = 5$  ns,  $\lambda = 1064$  nm) and a photomultiplier (Hamamatsu photonics, R5108, response time  $\leq 1.1$  ns). The Nd:YAG laser response was monitored with a digital oscilloscope (Sony Tektronix, TDS3052, 500 MHz) synchronized to the single-pulse excitation. The emission quantum yield excited at 355 nm ( $\Phi_{\pi-\pi^*}$ ) was estimated using a JASCO F-6300-H spectrometer attached with JASCO ILF-53 integrating sphere unit ( $\varphi = 100$  mm).

## References

- Hou, D. *et al.* Intense Blue Emission Phosphor  $\text{BaCa}_2\text{MgSi}_2\text{O}_8$ :  $\text{Eu}^{2+}$  for Fluorescent Lamps. *ECS J. Solid State Sci. Technol.* **2**, R79–R81 (2013).
- Kuo, T.-W., Huang, C.-H. & Chen, T.-M. Intense violet-blue-emitting  $\text{Ba}_2\text{AlB}_4\text{O}_9\text{Cl}:\text{Eu}^{2+}$  phosphors for applications in fluorescent lamps and ultraviolet-light-emitting diodes. *Appl. Opt.* **49**, 4202–4206 (2010).
- Huang, C.-H., Kuo, T.-W. & Chen, T.-M. Thermally stable green  $\text{Ba}_3\text{Y}(\text{PO}_4)_3:\text{Ce}^{3+}, \text{Yb}^{3+}$  and red  $\text{Ca}_3\text{Y}(\text{AlO})_3(\text{BO}_3)_4:\text{Eu}^{3+}$  phosphors for white-light fluorescent lamps. *Opt. Express* **19**, 238–241 (2011).
- Wang, J. *et al.* Solution-processible brilliantly luminescent  $\text{Eu}^{\text{III}}$  complexes with host-featured phosphine oxide ligands for monochromic red-light-emitting diodes. *Chem. Eur. J.* **20**, 11137–11148 (2014).
- Xu, H. *et al.* A unique white electroluminescent one-dimensional europium(III) coordination polymer. *J. Mater. Chem. C* **3**, 1893–1903 (2015).
- Ahmed, Z. & Iftikhar, K. Efficient photoluminescent complexes of 400–1800 nm wavelength emitting lanthanides containing organic sensitizers for optoelectronic devices. *RSC Adv.* **4**, 63696–63711 (2014).
- Xu, H., Zhu, R., Zhao, P. & Huang, W. Monochromic Red-Emitting Nonconjugated Copolymers Containing Double-Carrier-Trapping Phosphine Oxide  $\text{Eu}^{3+}$  Segments: Toward Bright and Efficient Electroluminescence. *J. Phys. Chem. C* **115**, 15627–15638 (2011).
- Ling, Q. *et al.* Non-Volatile Polymer Memory Device Based on a Novel Copolymer of N-Vinylcarbazole and Eu-Complexed Vinylbenzoate. *Adv. Mater.* **17**, 455–459 (2005).
- He, H. *et al.* Controllable synthesis of  $\text{Zn}_2\text{GeO}_4$ :Eu nanocrystals with multi-color emission for white light-emitting diodes. *J. Mater. Chem. C* **3**, 5419–5429 (2015).
- Rangari, V. V. & Dhoble, S. J. Synthesis and photoluminescence studies of  $\text{Ba}(\text{Gd}, \text{Ln})\text{B}_9\text{O}_{16}:\text{Eu}^{3+}$  ( $\text{Ln} = \text{La}, \text{Y}$ ) phosphors for n-UV LED lighting and display devices. *J. Rare Earths* **33**, 140–147 (2015).
- Du, P., Krishna Bharat, L. & Yu, J. S. Strong red emission in  $\text{Eu}^{3+}/\text{Bi}^{3+}$  ions codoped  $\text{CaWO}_4$  phosphors for white light-emitting diode and field-emission display applications. *J. Alloys Compd.* **633**, 37–41 (2015).
- Bellocchi, G., Fabbri, F., Miritello, M., Iacona, F. & Franzò, G. Multicolor Depth-Resolved Cathodoluminescence from Eu-Doped SiOC Thin Films. *ACS Appl. Mater. Interfaces* **7**, 18201–18205 (2015).
- Kumar, K. N., Vijayalakshmi, L. & Ratnakaram, Y. C. Energy transfer based photoluminescence properties of  $(\text{Sm}^{3+} + \text{Eu}^{3+})$ :PEO+PVP polymer films for Red luminescent display device applications. *Opt. Mater.* **45**, 148–155 (2015).
- Hasegawa, Y. Photofunctional Lanthanoid Complexes, Coordination Polymers, and Nanocrystals for Future Photonic Applications. *Bull. Chem. Soc. Jpn.* **87**, 1029–1057 (2014).
- Kanazawa, K., Nakamura, K. & Kobayashi, N. Electrochemical luminescence modulation in a Eu(III) complex-modified  $\text{TiO}_2$  electrode. *J. Mater. Chem. C* **3**, 7135–7142 (2015).
- Hirai, Y. *et al.* Luminescent Coordination Glass: Remarkable Morphological Strategy for Assembled Eu(III) Complexes. *Inorg. Chem.* **54**, 4364–4370 (2015).
- Hasegawa, Y. *et al.* Enhanced Electric Dipole Transition in Lanthanide Complex with Organometallic Ruthenocene Units. *J. Phys. Chem. A* **119**, 4825–4833 (2015).
- Daumann, L. J. *et al.* New Insights into Structure and Luminescence of Eu(III) and Sm(III) Complexes of the 3,4,3-Li(1,2-HOPO) Ligand. *J. Am. Chem. Soc.* **137**, 2816–2819 (2015).
- Reddy, M. L. P. & Sivakumar, S. Lanthanide benzoates: A versatile building block for the construction of efficient light emitting materials. *Dalton Trans.* **42**, 2663–2678 (2013).
- Ancel, L., Gateau, C., Lebrun, C. & Delangle, P. DNA Sensing by a Eu-Binding Peptide Containing a Proflavine Unit. *Inorg. Chem.* **52**, 552–554 (2013).
- Debroye, E. *et al.* Micellar self-assemblies of gadolinium(III)/europium(III) amphiphilic complexes as model contrast agents for bimodal imaging. *Dalton Trans.* **43**, 3589–3600 (2014).
- da Silva, F. F. *et al.* New lanthanide-CB[6] coordination compounds: relationships between the crystal structure and luminescent properties. *Dalton Trans.* **43**, 5435–5442 (2014).
- Pacold, J. I. *et al.* Direct Observation of 4f Intrashell Excitation in Luminescent Eu Complexes by Time-Resolved X-ray Absorption Near Edge Spectroscopy. *J. Am. Chem. Soc.* **136**, 4186–4191 (2014).
- Biju, S. *et al.* A Eu(III) Tetrakis( $\beta$ -diketonate) Dimeric Complex: Photophysical Properties, Structural Elucidation by Sparkle/AM1 Calculations, and Doping into PMMA Films and Nanowires. *Inorg. Chem.* **53**, 8407–8417 (2014).
- Caffrey, D. F. & Gunnlaugsson, T. Displacement assay detection by a dimeric lanthanide luminescent ternary Tb(III)-cyclen complex: high selectivity for phosphate and nitrate anions. *Dalton Trans.* **43**, 17964–17970 (2014).
- Biju, S., Eom, Y. K., Bunzli, J.-C. G. & Kim, H. K. Biphenylene-bridged mesostructured organosilica as a novel hybrid host material for  $\text{Ln}^{\text{III}}$  ( $\text{Ln} = \text{Eu}, \text{Gd}, \text{Tb}, \text{Er}, \text{Yb}$ ) ions in the presence of 2-thenoyltrifluoroacetone. *J. Mater. Chem. C* **1**, 3454–3466 (2013).
- Kitchen, J. A. *et al.* Circularly Polarized Lanthanide Luminescence from Langmuir-Blodgett Films Formed from Optically Active and Amphiphilic  $\text{Eu}^{\text{III}}$ -Based Self-Assembly Complexes. *Angew. Chem. Int. Ed.* **51**, 704–708 (2012).
- Neil, E. R., Funk, A. M., Yufit, D. S. & Parker, D. Synthesis, stereocontrol and structural studies of highly luminescent chiral triamidepyridyl-triazacyclononane lanthanide complexes. *Dalton Trans.* **43**, 5490–5504 (2014).
- Shelton, A. H., Sazanovich, I. V., Weinstein, J. a. & Ward, M. D. Controllable three-component luminescence from a 1,8-naphthalimide/Eu(III) complex: white light emission from a single molecule. *Chem. Commun.* **48**, 2749–2751 (2012).
- Bünzli, J.-C. G. On the design of highly luminescent lanthanide complexes. *Coord. Chem. Rev.* **293–294**, 19–47 (2015).
- Shavaleev, N. M., Eliseeva, S. V., Scopelliti, R. & Bünzli, J.-C. G. Tridentate Benzimidazole-Pyridine-Tetrazolates as Sensitizers of Europium Luminescence. *Inorg. Chem.* **53**, 5171–5178 (2014).
- Lehr, J., Beer, P. D., Faulkner, S. & Davis, J. J. Exploiting lanthanide luminescence in supramolecular assemblies. *Chem. Commun.* **50**, 5678–5687 (2014).
- Sykes, D. *et al.* Sensitisation of Eu(III)- and Tb(III)-based luminescence by Ir(III) units in Ir/lanthanide dyads: evidence for parallel energy-transfer and electron-transfer based mechanisms. *Dalton Trans.* **43**, 6414–6428 (2014).



34. Sykes, D. *et al.* d → f Energy Transfer in Ir(III)/Eu(III) Dyads: Use of a Naphthyl Spacer as a Spatial and Energetic ‘Stepping Stone’. *Inorg. Chem.* **52**, 10500–10511 (2013).
35. Eliseeva, S. V. & Bünzli, J.-C. G. Lanthanide luminescence for functional materials and bio-sciences. *Chem. Soc. Rev.* **39**, 189–227 (2010).
36. Zhang, H. *et al.* Highly luminescent and thermostable lanthanide-carboxylate framework materials with helical configurations. *J. Mater. Chem.* **22**, 21210–21217 (2012).
37. Lee, W. R. *et al.* Microporous Lanthanide-Organic Frameworks with Open Metal Sites: Unexpected Sorption Propensity and Multifunctional Properties. *Inorg. Chem.* **49**, 4723–4725 (2010).
38. Kataoka, H. *et al.* Photo- and thermo-stable luminescent beads composed of Eu(III) complexes and PMMA for enhancement of silicon solar cell efficiency. *J. Alloys Compd.* **601**, 293–297 (2014).
39. Hasegawa, Y. *et al.* Absorption cross-section control of Eu(III) complexes for increase of amplified spontaneous emission excited by third harmonic of nanosecond Nd:YAG laser. *J. Alloys Compd.* **488**, 578–581 (2009).
40. Miyata, K. *et al.* Thermostable Organo-phosphor: Low-Vibrational Coordination Polymers That Exhibit Different Intermolecular Interactions. *Chem Plus Chem* **77**, 277–280 (2012).
41. Friesen, C. M., Montgomery, C. D. & Temple, S. A. J. U. The first fluorine biphasic hydrogenation catalyst incorporating a perfluoropolyalkylether: [RhCl(PPh<sub>2</sub>(C<sub>6</sub>H<sub>4</sub>C(O)OCH<sub>2</sub>CF(CF<sub>3</sub>))(OCF<sub>2</sub>CF(CF<sub>3</sub>))<sub>n</sub>F)]<sub>3</sub> with n = 4–9. *J. Fluor. Chem.* **144**, 24–32 (2012).
42. Václavík, J. *et al.* AuI Catalysis on a Coordination Polymer: A Solid Porous Ligand with Free Phosphine Sites. *Chem Cat Chem* **5**, 692–696 (2013).
43. Hasegawa, Y. *et al.* Effect of Ligand Polarization on Asymmetric Structural Formation for Strongly Luminescent Lanthanide Complexes. *Eur. J. Inorg. Chem.* **2013**, 5911–5918 (2013).

## Acknowledgements

We appreciate for RIGAKU Co., Application Laboratories, Shimadzu Corporation, Mr. Nishino and Frontier Chemistry Center Akira Suzuki “Laboratories for Future creation” Project. This work was partly supported by Grants-in-Aid for Scientific Research on Innovative Areas of “New Polymeric Materials Based on Element-Blocks (no. 2401)” (no. 24102012) of the Ministry of Education, Culture, Sports, Science and Technology (MEXT), Japan. We appreciate for Shimadzu Corporation, Mr. Nishino and Frontier Chemistry Center Akira Suzuki “Laboratories for Future creation” Project.

## Author Contributions

A.N. performs the synthesis, measurements, and wrote the paper, A.N., T.N., Y.K., K.F., and Y.H. discussed and designed the research. T.S. and H.I. supported XRD measurements.

## Additional Information

**Supplementary information** accompanies this paper at <http://www.nature.com/srep>

**Competing financial interests:** The authors declare no competing financial interests.

**How to cite this article:** Nakajima, A. *et al.* Hyper-stable organo-EuIII luminophore under high temperature for photo-industrial application. *Sci. Rep.* **6**, 24458; doi: 10.1038/srep24458 (2016).



This work is licensed under a Creative Commons Attribution 4.0 International License. The images or other third party material in this article are included in the article’s Creative Commons license, unless indicated otherwise in the credit line; if the material is not included under the Creative Commons license, users will need to obtain permission from the license holder to reproduce the material. To view a copy of this license, visit <http://creativecommons.org/licenses/by/4.0/>